Nanopatterning of Mobile Lipid Monolayers on Electron-Beam-Sculpted Teflon AF Surfaces

Mehrnaz Shaali,[†] Samuel Lara-Avila,[‡] Paul Dommersnes,[§] Alar Ainla,[∥] Sergey Kubatkin,[‡] and Aldo Jesorka*[,†]

[†]Department of Chemical and Biological Engineering and [‡]Quantum Device Physics Laboratory, Chalmers University of Technology, 41296 Gothenburg, Sweden, [§]Department of Physics, Norwegian University of Science and Technology, N-7491 Trondheim, Norway, and [∥]Department of Chemistry and Chemical Biology, Harvard University, Cambridge, Massachusetts 02138, United States

ABSTRACT Direct electron-beam lithography is used to fabricate nanostructured Teflon AF surfaces, which are utilized to pattern surface-supported monolayer phospholipid films with 50 nm lateral feature size. In comparison with unexposed Teflon AF coatings, e-beam-irradiated areas show reduced surface tension and surface potential. For phospholipid monolayer spreading experiments, these areas can be designed to function as barriers that enclose unexposed areas of nanometer dimensions and confine the lipid film within. We show that the effectiveness of the barrier is defined by pattern geometry and radiation dose. This surface preparation technique represents an efficient, yet simple, nanopatterning strategy supporting studies of lipid monolayer behavior in ultraconfined spaces. The generated structures are useful for imaging studies of biomimetic membranes and other specialized surface applications requiring spatially controlled formation of self-assembled, molecularly thin films on optically transparent patterned polymer surfaces with very low autofluorescence.

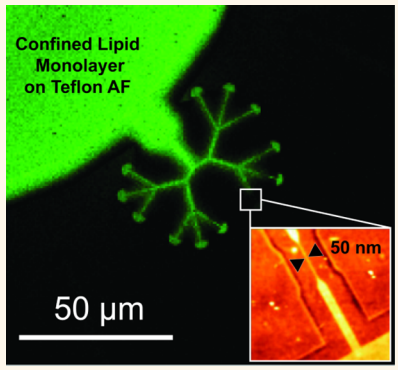

KEYWORDS: lipid monolayer · Teflon AF · nanofluidics · e-beam sculpting · lipid spreading

The design of 2D chemical reactors has been of considerable interest in recent years because the kinetics of chemical reactions depends on dimensionality.[1] Deeper understanding of fundamental mechanisms of molecular interactions can be achieved,[2] and the transport and reaction properties of individual molecules can be finely controlled and investigated.[3] The future development of ultrasmall devices critically relies on the ability to influence chemical reactions in nanoscopic confined environments. Examples of such developments include single-molecule separation devices,[4] nanosensors,[5] and molecular electronics.[6]

In several recent studies, chemical reactions in restricted geometries were investigated,[7−9] where a reduction of the third dimension to the nanometer length scale was achieved by various means, such as self-assembled soft matter nanotubes[10] and vesicles,[11] nanodroplets,[12] and fabricated nanofluidic devices.[4] The transition to truly 2D devices for the purpose of constructing a chemical reactor remains rather challenging because fluidity of the resulting molecular film, which is essential for transport, mixing, and interaction of reactants, needs to be assured. One promising approach to mobile molecular films involves self-assembled surfactant layers, in particular, phospholipid-based biomembranes stabilized by a support surface.[13] Supported phospholipid membrane devices are a common approach to fluidic nanoscale systems with reasonably simple preparation,[14] good transport properties, and high flexibility with respect to chemical functionality.[15]

In brief, at the solid−liquid interface, typically represented by an aqueous liquid phase interfacing a flat solid substrate, amphiphilic phospholipid molecules can be assembled to form continuous fluid films of nanometer thickness. The resulting film can be a monolayer, bilayer, or multilayer, depending on the preparation technique, the hydrophobicity of the surface, and the ionic strength of the surrounding solution.[16,17] Generally, if the surface is hydrophilic, a bilayer is formed, while hydrophobic (low-energy) surfaces lead to monolayer lipid films.[18,19]

* Address correspondence to aldo@chalmers.se.

Received for review September 9, 2014 and accepted December 26, 2014.

Published online December 26, 2014
10.1021/nn5050867

While most of the current research is focused on lipid bilayer architectures on a solid support,[20−23] there is a growing interest in monolayer film fabrication and use, primarily motivated by the biological importance of the monolayer. Interactions of lipids in monolayers with proteins are physiologically highly relevant. In the pulmonary system, a monolayer lipid film functions as a lubricant to assist inhalation and exhalation, where proteins regulate the process.[24,25] Monolayer lipids in the tear film of the eye protect it from drying.[26,27] Moreover, research on monolayers has contributed to the advancement of biophysical single-molecule studies[2] and generated new knowledge of phase behavior of lipids as well as mixed phases with other biologically active molecules, for example, cholesterol.[28,29] Distinct differences in structure and properties to bilayers and biological membranes have recently been highlighted.[30]

To generate supported lipid monolayers on hydrophobic surfaces, Langmuir−Blodgett assembly with subsequent film transfer deposition is the most commonly used technique.[13,31] Small vesicle fusion approaches have also been reported, although they remain rare exceptions.[21,32] In recent years, lipid film self-spreading techniques have been developed. In one of them, a multilamellar vesicle (MLV) is placed onto a low-energy solid surface submerged in aqueous buffer solution.[33] This leads to the gradual formation of a lipid film by rupturing the reservoir and the lipid self-spreading on the accessible surface, drawing lipid material from the MLV. Greater independency from solution conditions and better long-term stability of low-energy surfaces add some practical advantages to using supported lipid monolayers instead of bilayers to fabricate devices.[34,35]

We and others have previously studied the spreading of lipid monolayer on hydrophobic surfaces in detail and reported on suitable surface materials and techniques for their fabrication.[18,34−38] For example, we showed the possibility of confinement and mixing of mobile lipid monolayers on nano/micropatterned SU-8 surfaces,[33] controlled release of DNA molecules from decorated surface areas,[39] and temperature-controlled flow manipulation in spreading-based lipid devices.[38]

Among the different easily accessible low-energy surface materials, Teflon AF, a member of the amorphous fluoropolymer family, is a favorable choice. Teflon AF has low surface energy, high optical transmission, biocompatibility, and a low dielectric constant. It is chemically inert within wide boundaries and features superb thermal stability. In comparison to the chemically amplified photoresists SU-8 and EPON and other patternable low-energy surfaces, including polyacrylate e-beam resists such as poly(methyl methacrylate) (PMMA), Teflon AF exhibits much lower autofluorescence, which makes it a superior choice for biological studies involving fluorescence-based imaging techniques.[40−42]

However, micro- and nanopatterning of Teflon AF poses a considerable challenge. Currently available techniques for micropatterning of Teflon AF are mostly based on focused ion beam etching, synchrotron radiation, and laser light exposure, which are limited to micrometer resolution.[43−47] Common photolithography has also been reported as an alternative, allowing for micropatterning of Teflon AF surfaces with the smallest feature size of ~1 μm.[34]

To introduce nanosized features into a Teflon AF surface, Karre *et al.* employed electron-beam lithography on thin films of the material and achieved the smallest feature size of 200 nm.[48] This direct e-beam patterning does not form isolated individual structures but causes the formation of trenches with dose-dependent depth on the film surface.

In this study, we show that the extent of spreading of a lipid monolayer from a MLV source placed on Teflon AF can be limited and guided by patterns sculpted onto the surface by electron-beam (e-beam) exposure. We report that trenches formed on thin Teflon AF films (~50−75 nm) by e-beam irradiation are suitable to block and guide the propagation of a spreading lipid monolayer. Lipid films can be effectively confined within closed e-beam-written contours (Figure 2). This nanopatterning approach reduces the fabrication effort to the prewriting preparation steps, with no postprocessing such as developing, baking, etching, or lift-off required,[39] thus eliminating the sources of postexposure surface contamination. We further show how the front of a spreading lipid film can be guided into a lane of nanometer width, the contours of which we predefined on the surface. Our experiments demonstrate that spreading of lipid monolayers is possible in nanolanes as narrow as 50 nm, approaching the critical lane width where the energy gain from wetting the lane surface is equal to the energy loss induced by the edge tension of the lipid film.

RESULTS AND DISCUSSION

In a first set of experiments, lipid material was prepared and deposited onto e-beam-exposed and unexposed Teflon-AF-coated microscope coverslips, and their spontaneous spreading behavior was investigated. Figure 1a shows a multilamellar lipid vesicle (soybean polar extract phospholipid doped with 1% w/w lipid-conjugated fluorophore Texas Red) after deposition onto an e-beam-exposed (500 μC/cm^2) Teflon AF surface. The vesicle adheres to the surface, but lipid spreading was not observed, even after several hours. In contrast, on an unexposed Teflon AF surface, the deposited lipid spreads instantly after deposition of the vesicle in an isotropic manner (Figure 1b), with a spreading coefficient and diffusion constant in accordance with previous findings.[38]

This initial result suggested that bulk surface properties of the coating are relevant for lipid film propagation and are significantly influenced by the e-beam treatment. This led us to further investigate utilization of e-beam-exposed areas as a functional barrier to stop lipid spreading and confine the lipid in enclosed regions on the unexposed Teflon AF surface and also to define pathways through which spreading can be guided. Figure 2 illustrates the concept of a lipid monolayer spreading device based on e-beam-patterned Teflon AF.

The areas depicted in black correspond to the surface that has been irradiated in order to confine the lipid to the encircled area. Our experimental pattern is composed of a large circular body, in which the lipid material can be deposited, and eight arms with branching lanes of different widths and lengths, ranging from 250 to 50 nm as the smallest enclosed feature size. The constrictions in each arm are 2 μm (left main branch) and 5 μm (right main branch) long. The body where the lipid vesicle is deposited by the microtransfer technique[33] was designed to be large enough to allow for facile vesicle transfer by means of a glass microneedle with an opening of $\sim$1 μm. Each of the eight lanes is 10 μm at their widest part and becomes gradually narrower toward their final width. At the end of each lane, we created a small control pool, which was established to facilitate the monitoring of lipid spreading through the lanes. The central area is defined by exposing a border area of 10 μm width. In addition, the entire space between the branches was exposed. A 1 μm wide area around the narrow constrictions was exposed first with a lower beam current in order to avoid exposure of the nanolanes. (Note: arrow 4 in Figure 4f points to the interface between the two differently exposed areas, where slightly increased fluorescence intensity is noticeable.) For the functioning of the device, it is, in principle, sufficient to expose only a thin frame of 1 μm width around the constrictions and end reservoirs.

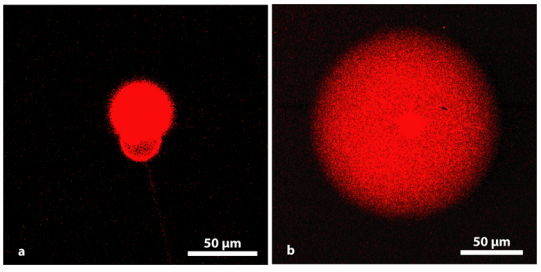

Figure 1. (a) Multilamellar lipid vesicle with an attached unilamellar vesicle deposited on an e-beam-exposed Teflon AF surface (dose: 500 μC cm^{-2}). No spreading was observed after 2 h. (b) Multilamellar lipid vesicle spreads within 5 min after it is deposited onto the Teflon AF surface.

After patterning of Teflon AF by e-beam lithography, we performed atomic force microscopy (AFM) characterization of the surface. The topography information reveals the formation of $\sim$7 nm deep trenches in Teflon AF upon e-beam exposure (Figure 3a).

The characterization of the Teflon AF surfaces was complemented by surface potential measurements. In Figure 3b,c, we present tapping mode AFM and Kelvin probe force microscopy images of adjacent areas of exposed and unexposed Teflon, respectively. The surface potential difference is on the order of 120 mV, which remains constant, independent from the applied e-beam dose in the range covered in this study.

The depth of the trenches, however, displays a strong dose dependency (Figure 3d). A 5-fold increase in exposure dose causes almost a doubling of the trench depth from 4 to 7 nm, which is comparatively large when considering the thickness of a lipid monolayer of $\sim$1−2 nm. For the given thickness of the Teflon AF film, exposure doses greater than 1500 μC cm^{-2} did not cause further changes, neither in trench depth nor in surface potential (data not shown). Note that Karre *et al.* also reported a dependency of trench depths on the total thickness of the Teflon AF film.[48]

X-ray photoelectron spectroscopy (XPS) oxygen analysis revealed further clues with respect to the chemical modifications in the polymer following e-beam irradiation. Our experiments show the appearance of a

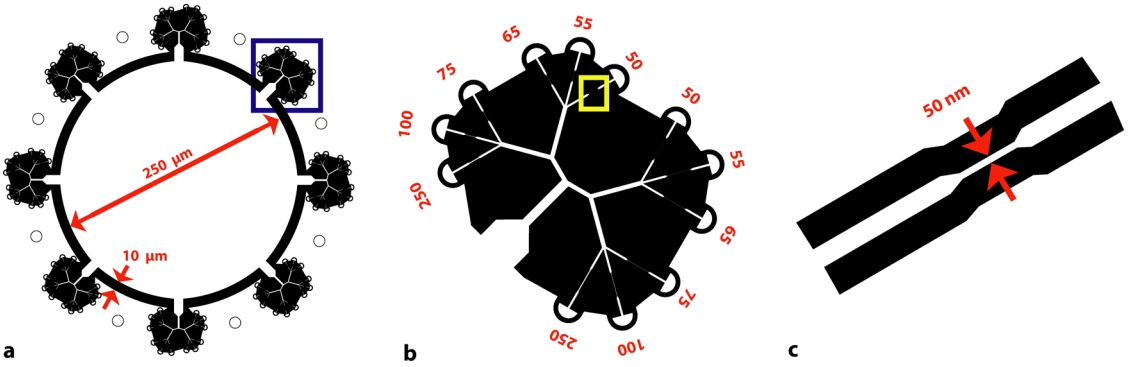

Figure 2. (a) Geometry of the lipid spreading device. The black areas are exposed by the electron beam. (b) Enlarged view of one of the branches (blue square) with their terminating collection pools. The numbers in the drawing denote the designed width of the corresponding nanolane. (c) Close-up view of the smallest, 50 nm wide, lane (yellow square).

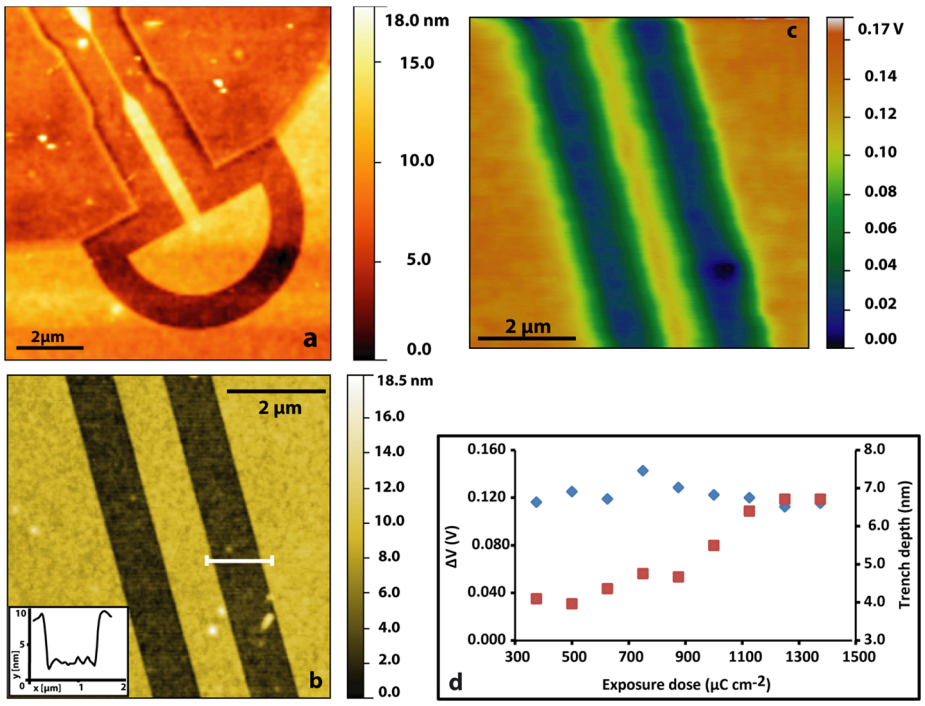

Figure 3. (a) AFM topography image of the Teflon AF surface after e-beam exposure. (b) Kelvin probe force microscopy image of the e-beam-exposed frame. (c) AFM topography image of (b). (d) Dose dependency of the surface potential (blue diamonds) and trench depth (red squares).

new energy peak around 533 eV, indicating the formation of double bonds between C and O in a fraction of the polymer molecules. This suggests the formation of keto or carboxylic acid groups, possibly arising from a rearrangement of the dioxole moiety in the fluoropolymer. More elaborate determinations of the surface structure are underway. Our XPS measurements are in agreement with Popovici *et al.*,[49] who demonstrated that irradiating Teflon AF with Mg Kα radiation at 1253.6 eV leads to the degradation of the polymer and formation of C═O (Supporting Information SI2).

Independently conducted water contact angle measurements on larger areas showed a decrease from 118 to 94° for as-spun and irradiated surfaces, respectively (Supporting Information SI1). The structural changes in the irradiated film clearly cause a loss of lipophilicity, which we found to be sufficient to hinder the spreading of lipid films, so that selective coverage of the surface by the lipid film is observed. According to Karre *et al.*, electron radiation causes degradation of the polymer by removing some $-CF_3$ groups,[48] which explains to some extent the observed loss of hydrophobicity.

The spreading of phospholipid films in the e-beam-patterned surface regions was investigated by monitoring the fluorescence signal arising from fluorophores attached to a small percentage (1% w/w) of the lipids. Confocal microscopy was utilized for that purpose. After deposition of multilamellar vesicle to the surface, the lipid film was found to spread in a circular manner until it reached the exposed barrier. At this point, radial spreading nearly halted. When exit lanes were defined at the periphery (cf. Figure 2), film propagation continued only through the lanes, eventually filling up the terminating pools (Figure 4).

In order to verify that the lipid film that fills the entire pattern is due to spreading from the main vesicle deposited on the body, and not from lipid material that might be present in the aqueous medium (through-solution transfer), we designed isolated areas outside the main pattern, which were separated from the main surface through an exposed circular frame. The fact that these confined regions remained unfilled during the course of the entire experiment confirms the absence of lipid deposition through the surrounding medium (Supporting Information SI3).

To independently confirm that the e-beam-exposed areas are unfavorable for lipid monolayer formation, we performed two separate studies. In the first, fluorescence recovery after photobleaching (FRAP) experiments were performed on the exposed area, revealing that the lipid mobility in these exposed surface regions is significantly reduced (~2 orders of magnitude). In another auxiliary experiment, a fluorescently labeled small unilamellar vesicle suspension (SUVs, diameter 100 nm) was placed atop a freshly prepared e-beam-patterned Teflon AF surface. Fluorescence microscopy showed that the SUVs coat all unexposed Teflon AF areas spontaneously, but e-beam-exposed areas remained unaffected (Supporting Information S7).

We further observed that the pools are not populated equally fast. For branches of identical length,

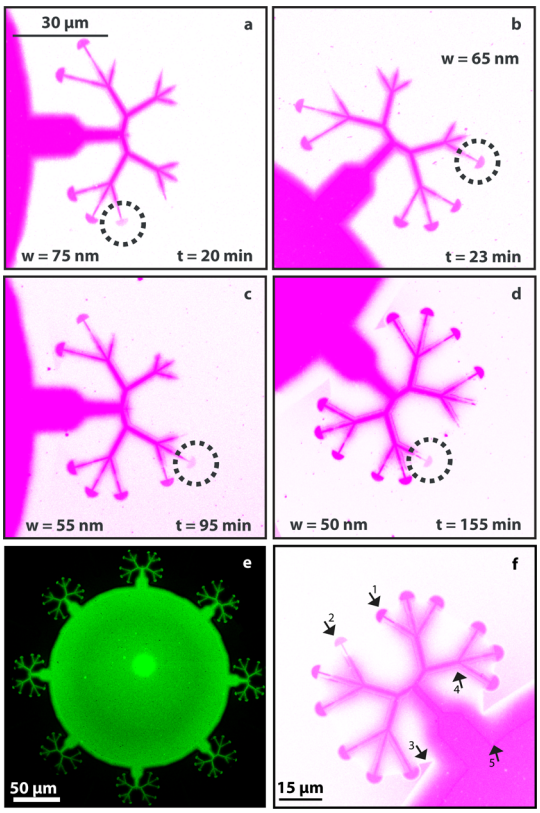

Figure 4. (a–d) Confocal image of one of the branches of the pattern depicted in Figure 2, demonstrating the lipid spreading in Teflon AF areas confined by e-beam exposure. The images were recorded at 20 (a), 23 (b), 95 (c), and 155 min (d) after deposition of the MLV. The lipid was doped with the fluorophore ATTO 488 (1% w/w). The dotted circle highlights the end pool which has just been filled at the time of recording. (e) Confocal image of the entire structure under investigation, recorded after 185 min. (f) Magnified view of one of the branches after 185 min of spreading time, with arrows highlighting specific features discussed in the main text. Arrows 1 and 2 point to the pools at the end of the narrowest (50 nm) lanes filled by the lipid, confirming that lipid spreading occurs through the constrictions of 2 and 5 μm length, respectively. Arrow 3 points to a site where lipid leaks through the barrier, due to reduced frame width (pattern design). Arrow 4 points to the interface between the areas of different exposure doses around the constrictions. Arrow 5 points to an area of increased fluorescence intensity in the frame region, possibly due to a specific interaction of the lipid-conjugated dye moiety with the exposed surface. (The images are inverted for better contrast.)

the time required to reveal lipid spreading in the terminating areas increased with decreasing lane width, but only for lane widths below 65 nm. At lane widths above 65 nm, the pools filled nearly equally fast. Compared to the wider lanes, the time demand for lanes narrower than 65 nm increased dramatically from a few minutes to hours. This indicates that wetting of the narrow exposed areas is still associated with an energy gain, with respect to the lysis tension of the lipid reservoir. The increased time requirement arises from an increased flow resistance and a smaller energy gain by wetting the surface in the constrictions, as compared to the wider areas (cf. discussion below).

The time series in Figure 4a,d, where the 75, 65, 55, and 50 nm lanes in the shorter (2 μm *vs* 5 μm) of the two sub-branches are highlighted by a dotted circle, depicts the sequential filling according to lane width. The behavior of the longer sub-branch is similar, although the 55 and 50 nm lanes remain unfilled even after 155 min. All pools in the 2 μm sub-branch were filled at the end of the series, although some differences became apparent.

During prolonged spreading, we observed that a fraction of the expanding lipid film crosses the confining frame, which in this experiment was 10 μm wide (Figure 2a). This is apparent in the time series shown in Figure 4, where increasing "fuzziness" of the borders of the expanding film can be observed in the frame regions, although the ends of those branches, where spreading is still progressing, remain sharp (Figure 4e, f). Arrows 1 and 2 point the end pools of the 50 nm lanes in the 2 and 5 μm sub-branches, respectively, which are filled last. Note that the comparatively higher fluorescence intensity seen in end pool 1 is an artifact. It is due to photobleaching of the surrounding areas in earlier confocal scans.

We also noted an increase in fluorescence intensity in the frame region (arrow 5 in Figure 4f). A separate investigation showed that the fluorescence intensity of the lipid film in the frame region is by a factor of ~1.5 higher than for the membrane spreading on unexposed Teflon AF (Supporting Information SI3). We rule out the possibility that the monolayer folds into a bilayer, which could occur due to the increased hydrophobicity. However, in such a case, the intensity should be consistently twice as large as the intensity value for monolayer fluorescence if we assume that the distribution of dye remains the same in both the upper and the lower leaflets. Our observation that the lipid does not stop on the far side of the barrier, but continues spreading as a monolayer, supports this conclusion (arrow 3 in Figure 4f). Moreover, the edge thinning typical for monolayer spreading on Teflon AF is still clearly visible on the exposed frame (Figure 4f). It remains to be established if the dye label interacts in some way with the exposed surface, so that a filtering effect leads to the accumulation of the labeled lipids on the frame regions. Dye charge and size might have an influence on this behavior, which has so far not been further investigated.

From the lipid spreading experiments, we also learned that the depth of the trench and the width of the frame have a pronounced influence on the capability of the border to restrict lipid flow. We determined that if the trench depth is <5 nm, corresponding to a dose <1125 μC cm^{-2}, the exposed Teflon AF is not capable of preventing the lipid film from crossing it. This is particularly interesting given that a dose as low as 500 μC cm^{-2} already prevents the disintegration of a multilamellar vesicle on an exposed surface (Figure 1a).

Trench depth and exposure dose may not be the only factors of importance. The water contact angle of exposed Teflon AF (94°, cf. Supporting Information SI1) is between those of the epoxy resists SU-8 (91°) and EPON (69°) and unexposed Teflon AF (118°). EPON shows considerably greater hydrophilicity but still permits monolayer spreading. In contrast, fluorocarbon layers deposited by plasma treatment of perfluorocyclobutane are strongly hydrophobic (115°) but do not support spreading. This indicates that, in addition to surface tension and its hydrophobicity, other factors like roughness and potential of the surface should be considered.[38,50] Our surface probe microscopy data show that the exposed areas have a lower surface potential (Figure 3c) but at the same time have reduced roughness (Supporting Information SI4). For the situation shown in Figure 1a, increased repulsion between the bulk negatively charged membranes in the initially present multilamellar reservoir and the comparatively more negatively charged exposed surface might hinder vesicle lysis as well as transformation from the bilayer membrane to a monolayer film, even though the energy gain obtained from wetting would exceed the lysis tension. On the other hand, when a monolayer has already formed (Figure 4; also cf. Supporting Information SI3), spreading in the exposed areas may occur, facilitated by the smoother surface. Considering the fact that the more exposed areas feature deeper trenches, which indicates more severe chemical/structural changes in the Teflon AF, a combination of both topography and chemical structure in the exposed areas is likely responsible for the reduced propagation of the lipid film.

In cases where there is sufficient unexposed area available to the lipid film to expand, the tendency of crossing the exposed barrier is greatly reduced. In contrast, if the available unexposed area is nearly filled, which is the case when the film has reached the subbranches where the nanoscale restrictions are located, the reduced surface free energy gain attained by wetting the exposed areas outweighs the gain from wetting the nanolane (constricted) areas. We cannot, however, exclude that at these small dimensions some lipid could cross the boundaries of the nanochannels and escape confinement. Possible considerations are that the chemical boundaries are not sharply defined (cf. Figure 3c) or that the lipids cross the boundary in order to reach a dynamic equilibrium between unfavorable surface energy and entropy of confinement.

The spreading of lipid monolayers on surfaces is driven by surface adhesion energy, and the kinetics is determined by the frictional dissipation (sliding friction) between the surface and the film. This is expressed by the spreading coefficient $\beta = \sigma_{adh}/2\zeta$, where σ_{adh} is the adhesion energy per unit area and ζ is the sliding friction coefficient.[33] The spreading coefficient in this description does not depend on lane width, which is in agreement with observations of lipid film spreading on micron-sized lanes.[39] This model does not, however, take into account boundary energies, which are relatively weak for large area films, but may become important when the film boundary to area ratio becomes large, for example, for nanosized lanes. The surface energy for the lipid film covering a lane is $E = -\sigma_{adh}wL + 2\gamma_e L$, where w is the lane width, L the lane length, σ_{adh} the adhesion energy, and γ_e the edge tension (boundary energy). The corresponding spreading coefficient is $\beta = (\sigma_{adh} - 2\gamma_e/w)/2\zeta$; for a critical lane length, $w_{crit} = 2\gamma_e/\sigma_{adh}$, the energy gain from wetting the lane surface is equal to the energy loss induced by the edge tension of the lipid film, and spreading is no longer energetically favorable. If w approaches w_{crit}, spreading will slow significantly and eventually come to a halt. It is reasonable to assume that γ_e of the monolayer is on the same order of magnitude as the edge tension of bilayer membranes, that is, between 1 and 50 pN. Assuming further that the σ_{adh} of Teflon AF has to be larger than the lysis tension of the reservoir, which is about 1−10 mN m^{-1} (spreading-induced tension in a bilayer membrane is close to 1 mN m^{-1}),[50] we find that w_{crit} is on the order of a few tens of nanometers (*e.g.* w_{crit} = 10 nm for γ_e = 25 pN and σ = 5 mN m^{-1}), which is close to our observation. Considering the time required for the spreading lipid film to cross different nanosized lane constrictions, which we obtained by monitoring the fluorescence intensity inside the terminating pool areas, we were able to estimate an upper limit for the critical lane width and the associated film edge tension. Above a lane width of 65 nm, the time required to cross the 2 μm long constrictions was on the order of 20 min (Figure 4a,b). A much longer time, on the order of 95−160 min, was required to cross the 55 and 50 nm constrictions (Figure 4c,d). It is therefore reasonable to assume that the critical lane width lies somewhere between 10 and 50 nm. It is also probable that other factors contribute to the reduced spreading velocity observed with narrow lane widths. Surface roughness and local defects could become more important since the polymer film is not infinitely smooth. A critical force F_{crit} may be required for the lipid to pass the nanoconstriction, and microscopic membrane viscosity most likely becomes important at small lane widths, slowing the spreading. For broader lanes, surface−monolayer friction (*i.e.*, slip velocity) dominates the spreading of surfactant monolayers. However, for very small line widths, membrane viscosity can contribute to slow the spreading. The crossover scale, where membrane viscosity becomes more important than sliding friction, is given by the characteristic length (which is the length scale where friction forces are on the same order as the viscous forces) $L_c = (\eta/\zeta)^{1/2}$, where η is the 2D viscosity of the lipid film and ζ is the surface−monolayer friction. If there is pinning to the lane edge, the 2D

film viscosity can play a role. If there is no pinning to the edge, the 2D viscosity is irrelevant because the flow of surfactants will be a "plug flow", that is, featuring no shear and no viscous dissipation.

A few additional points can be finally discussed. We also found that there is a minimum width of the trench, required for confining the spreading lipid sufficiently for practical purposes, of ~10 μm (Supporting Information SI3). The need for a sufficiently extensive frame area should be kept in mind if it is desired to separate spreading lanes from each other, for example, when different lipid sources are to be deposited in different confined areas on the surface. Cross-contamination can effectively be avoided in such cases by designing the pattern to leave a large enough distance between individual spreading areas.

Arrow 3 in Figure 4f highlights a rather disadvantageous design feature in the presented chip layout, which we have not removed, as it demonstrates that lipid spreading continues as a monolayer after crossing the exposed border. It also illustrates that an exposed border of at least 10 μm width is beneficial in membrane spreading experiments utilizing lanes with 50 nm feature size. The triangular section in the area between the branches and the circular body, to which the arrow points, reduces the width of the exposed periphery from 10 to ~5 μm. At such an incursion point, lipid preferentially breaks through the barrier. The fluorescence intensity gradients seen in Figure 4f, emanating from the tip of the triangular areas to both sides of the branch, indicate that the lipid material, which has escaped its confinement and contaminates the surface outside the exposed frame, originates from these point sources.

In conclusion, we have presented an innovative fabrication route to micro- and nanopatterend surfaces coated with the polymer, which allows for confining lipid monolayers in predefined surface regions. Since these lipid films are mobile and tend to cover the available surface until the accessible lipid material is distributed, the new patterned surfaces can be utilized to direct spreading of such films along desired paths. The patterning method, essentially the preparation of a frame around the desired regions, is a simple procedure that does not require (apart from surface spin-coating and exposure) any postexposure treatment or chemical development. A number of factors influence the effectiveness of the lipid confinement, most notably the width of the frame and the exposure dose, but spreading lane width and length are also of importance. In conclusion, a width of 10 μm at an exposure dose >1200 μC cm^{-2} is sufficient to hold back the lipid that is propagating in spreading lanes of 50 nm width. The time required for this process is on the order of hours, which is comparatively long but may be alleviated by a more suitable layout, for example, with shorter nanolanes. In-depth surface characterization revealed that the electron-beam-irradiated area is more hydrophilic and negatively charged in comparison with the unexposed Teflon AF surface.

This technique can be applied as a nanostructuring protocol to control monolayer lipid spreading through nanoscale constrictions with very well-defined geometry, useful particularly as a platform for single-molecule studies. The interesting finding that vesicles adhere but do not spread on exposed areas might open possibilities to employ such surfaces in application that involve immobilization of intact vesicles, possibly in the context of surface-adhered vesicle−nanotube networks,[51] where it could replace the strongly autofluorescent SU-8, which is typically used as a remedy for the self-spreading problem.[52]

A so far unmentioned aspect of Teflon-AF-coated microscopy coverslips is their exceptionally long shelf life. The previously used SU-8-coated surfaces[33] show a decrease in spreading coefficient already after several weeks, whereas we have found that patterned Teflon AF surfaces in sealed containers maintain their properties over several months.

Future experimental work on the exposed surfaces should be directed toward lipid monolayer applications. However, more elaborate studies of the chemical properties of the exposed patches might reveal the presence of reactive groups, which are potentially interesting for chemical conjugation of molecules to the Teflon AF film. In this context, we plan to perform comparative studies on Teflon AF 2400, which has higher contents of dioxole functionalities.

MATERIALS AND METHODS

Equipment. The electron-beam lithography system (JEOL JBX-9300FS from JEOL (Tokyo, Japan)) was used as the radiation source for exposure. The deposition of alignment marks, which were introduced to facilitate locating the exposed areas under the microscope, was performed with an electron-beam evaporator (AVAC- HVC600, New York). A dry plasma etching system (BatchTop PE/RIE m/95, PlasmaTherm/Advanced Vacuum, USA) was used for pretreatment of the substrates. The tapered glass micropipettes for lipid transfer to the spreading areas on the substrates were prepared from GC100-TF borosilicate capillaries (Harvard Apparatus), using a micropipette laser puller (model P-2000, Sutter Instrument Co, Novato, USA). A Celltram Vario Pump (Eppendorf AG, Hamburg, Germany) was used to control the injection pressure in the micropipette during lipid deposition. To hold and move the micropipette under the microscope, a hydraulic micromanipulator system (MWH-3 and MC-35A, Narishige, Tokyo, Japan) was used. Standard clean-room fabrication methods and equipment were used for common substrate preparation steps, including cleaning, spin-coating, baking, and solvent work.

Microscopy. A Leica DM-IRE2 confocal microscope (Leica TCS SP2 RS) with a 40× oil objective with a NA of 1.25 was used to conduct confocal imaging experiments. Atomic force

microscopy was performed using a Veeco Dimension 3100 SPM scanning probe microscope in tapping mode (Veeco, New York, USA) with a NSG10 DLC probe (NT-MDT Europe BV, The Netherlands). The surface potential studies (Kelvin probe force microscopy) were conducted using a Dimension ICON SPM (Bruker, Masachusettes, USA). XPS was conducted using a Quantum 2000 scanning ESCA microprobe (Physical Electronics, Minnesota, USA).

Substrate Fabrication. The indium−tin oxide (ITO) substrates CEC020T (unbeveled borosilicate glass substrates, diameter = 50 mm (±0.25) × 50 mm (±0.25); thickness = 0.175 mm (±0.015), coated with ITO (20 ± 5 Ohms/sq)), obtained from Präzisions Glas & Optik (Iserlohn, Germany), were rinsed in acetone followed by isopropyl alcohol. To remove possible organic contaminants, the substrate was plasma treated with oxygen (10 sccm oxygen, 500 mbar, 50 W) for 10 min. To improve the adhesion of Teflon AF to the substrate, hexamethyl disilazane from Micro Resist Technology GmbH (Berlin, Germany) was spin-coated onto the substrate (3000 rpm) and baked on a hot plate (110 °C for 90 s). Teflon AF1600 (poly[4,5-difluoro-2,2-bis(trifluoromethyl)-1,3-dioxole-*co*-tetrafluoroethylene]) solution (grade 601S2-100-6 1600 with 6% (w/w) solids contents based on Teflon AF1600, glass transition temperature T_g = 160 °C) was obtained from Dupont Chemicals (Wilmington, USA). It was first diluted with FC-40 (CAS 51142-49-5, Sigma-Aldrich, Missouri, USA) to 1.2% w/w. The diluted solution was spin-coated onto the substrate (2000 rpm) to reach ∼60 nm final thickness and baked for 15 min at 180 °C, passing the glass transition temperature of Teflon AF. The substrate was then loaded into the electron-beam lithography system, where it was exposed using a predesigned pattern. The pattern was designed with standard drawing software (AutoCad 2007, AutoDesk Inc.). The applied electron-beam acceleration voltage was 100 kV; the beam current was 40 nA (1 nA for a 1 μm frame around the narrow constrictions), and the exposure doses were chosen in the range between 375 and 1500 μC cm^{-2}.

Lipid Preparation. A mixture of 99% soybean polar extract phospholipid (Avanti Polar Lipids) and 1% w/w lipid-conjugated fluorophore TexasRed/1,2-dihexadecanoyl-*sn*-glycero-3-phosphoethanolamine triethylammonium salt or ATTO 488/1,2-dioleoyl-*sn*-glycero-3-phosphoethanolamine (Invitrogen, Stockholm, Sweden) was used to prepare multilamellar vesicles by the dehydration and rehydration method.[51]

Confocal Imaging. After exposure, the substrate was placed onto the stage of the confocal microscope. A droplet of phosphate buffer solution was deposited on top of the patterned surface area. By applying the microtransfer technique,[53] a multilamellar lipid vesicle was deposited onto the center of a pattern, and the spreading process was monitored by confocal microscopy.

Conflict of Interest: The authors declare no competing financial interest.

Acknowledgment. We thank A. Wendel for help with the XPS studies. We acknowledge the Nordic Network for Dynamic Biomembrane Research, The Chalmers Area of Advance in Nanoscience and Technology, and the Swedish Research Council (VR).

Supporting Information Available: Water contact angle measurements, XPS spectra of exposed and unexposed Teflon AF, additional confocal images, the roughness study by AFM, FRAP data on the lipid mobility in the exposed areas and data on the interaction of the surfaces with nanovesicles. This material is available free of charge *via* the Internet at http://pubs.acs.org.

REFERENCES AND NOTES

1. Savageau, M. A. Michaelis−Menten Mechanism Reconsidered: Implications of Fractal Kinetics. *J. Theor. Biol.* **1995**, *176*, 115–124.
2. Hannestad, J. K.; Brune, R.; Czolkos, I.; Jesorka, A.; El-Sagheer, A. H.; Brown, T.; Albinsson, B.; Orwar, O. Kinetics of Diffusion-Mediated DNA Hybridization in Lipid Monolayer Films Determined by Single-Molecule Fluorescence Spectroscopy. *ACS Nano* **2013**, *7*, 308–315.
3. Nabika, H.; Sasaki, A.; Takimoto, B.; Sawai, Y.; He, S.; Murakoshi, K. Controlling Molecular Diffusion in Self-Spreading Lipid Bilayer Using Periodic Array of Ultra-small Metallic Architecture on Solid Surface. *J. Am. Chem. Soc.* **2005**, *127*, 16786–16787.
4. Xia, D. Y.; Yan, J. C.; Hou, S. F. Fabrication of Nanofluidic Biochips with Nanochannels for Applications in DNA Analysis. *Small* **2012**, *8*, 2787–2801.
5. Dittrich, P. S.; Manz, A. Lab-on-a-Chip: Microfluidics in Drug Discovery. *Nat. Rev. Drug Discovery* **2006**, *5*, 210–218.
6. Ratner, M. A Brief History of Molecular Electronics. *Nat. Nanotechnol.* **2013**, *8*, 378–381.
7. Lizana, L.; Bauer, B.; Orwar, O. Controlling the Rates of Biochemical Reactions and Signaling Networks by Shape and Volume Changes. *Proc. Natl. Acad. Sci. U.S.A.* **2008**, *105*, 4099–4104.
8. Sott, K.; Lobovkina, T.; Lizana, L.; Tokarz, M.; Bauer, B.; Konkoli, Z.; Orwar, O. Controlling Enzymatic Reactions by Geometry in a Biomimetic Nanoscale Network. *Nano Lett.* **2006**, *6*, 209–214.
9. Benichou, O.; Chevalier, C.; Klafter, J.; Meyer, B.; Voituriez, R. Geometry-Controlled Kinetics. *Nat. Chem.* **2010**, *2*, 472–477.
10. Karlsson, R.; Karlsson, A.; Ewing, A.; Dommersnes, P.; Joanny, J. F.; Jesorka, A.; Orwar, O. Chemical Analysis in Nanoscale Surfactant Networks. *Anal. Chem.* **2006**, *78*, 5960–5968.
11. Christensen, S. M.; Bolinger, P. Y.; Hatzakis, N. S.; Mortensen, M. W.; Stamou, D. Mixing Subattolitre Volumes in a Quantitative and Highly Parallel Manner with Soft Matter Nanofluidics. *Nat. Nanotechnol.* **2012**, *7*, 51–55.
12. Edgar, J. S.; Milne, G.; Zhao, Y. Q.; Pabbati, C. P.; Lim, D. S. W.; Chiu, D. T. Compartmentalization of Chemically Separated Components into Droplets. *Angew. Chem., Int. Ed.* **2009**, *48*, 2719–2722.
13. Czolkos, I.; Jesorka, A.; Orwar, O. Molecular Phospholipid Films on Solid Supports. *Soft Matter* **2011**, *7*, 4562–4576.
14. Ainla, A.; Gozen, I.; Hakonen, B.; Jesorka, A. Lab on a Biomembrane: Rapid Prototyping and Manipulation of 2D Fluidic Lipid Bilayer Circuits. *Sci. Rep.* **2013**, *3*, 2743.
15. Castellana, E. T.; Cremer, P. S. Solid Supported Lipid Bilayers: From Biophysical Studies to Sensor Design. *Surf. Sci. Rep.* **2006**, *61*, 429–444.
16. Girard-Egrot, A. P.; Marquette, C. A.; Blum, L. J. Biomimetic Membranes and Biomolecule Immobillisation Strategies for Nanobiotechnology Applications. *Int. J. Nanotechnol.* **2010**, *7*, 753–780.
17. Richter, R. P.; Berat, R.; Brisson, A. R. Formation of Solid-Supported Lipid Bilayers: An Integrated View. *Langmuir* **2006**, *22*, 3497–3505.
18. Sanii, B.; Parikh, A. N. Surface-Energy Dependent Spreading of Lipid Monolayers and Bilayers. *Soft Matter* **2007**, *3*, 974–977.
19. Radler, J.; Strey, H.; Sackmann, E. Phenomenology and Kinetics of Lipid Bilayer Spreading on Hydrophilic Surfaces. *Langmuir* **1995**, *11*, 4539–4548.
20. Jung, M.; Vogel, N.; Koper, I. Nanoscale Patterning of Solid-Supported Membranes by Integrated Diffusion Barriers. *Langmuir* **2011**, *27*, 7008–7015.
21. Lenz, P.; Ajo-Franklin, C. M.; Boxer, S. G. Patterned Supported Lipid Bilayers and Monolayers on Poly(dimethylsiloxane). *Langmuir* **2004**, *20*, 11092–11099.
22. Morigaki, K.; Baumgart, T.; Offenhausser, A.; Knoll, W. Patterning Solid-Supported Lipid Bilayer Membranes by Lithographic Polymerization of a Diacetylene Lipid. *Angew. Chem., Int. Ed.* **2001**, *40*, 172–174.
23. Groves, J. T.; Boxer, S. G. Micropattern Formation in Supported Lipid Membranes. *Acc. Chem. Res.* **2002**, *35*, 149–157.
24. Ding, J. Q.; Takamoto, D. Y.; von Nahmen, A.; Lipp, M. M.; Lee, K. Y. C.; Waring, A. J.; Zasadzinski, J. A. Effects of Lung Surfactant Proteins, SP-B and SP-C, and Palmitic Acid on Monolayer Stability. *Biophys. J.* **2001**, *80*, 2262–2272.
25. Baoukina, S.; Tieleman, D. P. Lung Surfactant Protein SP-B Promotes Formation of Bilayer Reservoirs from Monolayer

and Lipid Transfer between the Interface and Subphase. *Biophys. J.* **2011**, *100*, 1678–1687.
26. Bron, A. J.; Tiffany, J. M.; Gouveia, S. M.; Yokoi, N.; Voon, L. W. Functional Aspects of the Tear Film Lipid Layer. *Exp. Eye Res.* **2004**, *78*, 347–360.
27. Kulovesi, P.; Telenius, J.; Koivuniemi, A.; Brezesinski, G.; Rantamaki, A.; Viitala, T.; Puukilainen, E.; Ritala, M.; Wiedmer, S. K.; Vattulainen, I.; et al. Molecular Organization of the Tear Fluid Lipid Layer. *Biophys. J.* **2010**, *99*, 2559–2567.
28. Weis, R. M. Fluorescence Microscopy of Phospholipid Monolayer Phase-Transitions. *Chem. Phys. Lipids* **1991**, *57*, 227–239.
29. Kewalramani, S.; Hlaing, H.; Ocko, B. M.; Kuzmenko, I.; Fukuto, M. Effects of Divalent Cations on Phase Behavior and Structure of a Zwitterionic Phospholipid (DMPC) Monolayer at the Air−Water Interface. *J. Phys. Chem. Lett.* **2010**, *1*, 489–495.
30. Watkins, E. B.; Miller, C. E.; Liao, W. P.; Kuhl, T. L. Equilibrium or Quenched: Fundamental Differences between Lipid Monolayers, Supported Bilayers, and Membranes. *ACS Nano* **2014**, *8*, 3181–3191.
31. Vontscharner, V.; McConnell, H. M. Physical-Properties of Lipid Monolayers on Alkylated Planar Glass Surfaces. *Biophys. J.* **1981**, *36*, 421–427.
32. Lingler, S.; Rubinstein, I.; Knoll, W.; Offenhausser, A. Fusion of Small Unilamellar Lipid Vesicles to Alkanethiol and Thiolipid Self-Assembled Monolayers on Gold. *Langmuir* **1997**, *13*, 7085–7091.
33. Czolkos, I.; Erkan, Y.; Dommersnes, P.; Jesorka, A.; Orwar, O. Controlled Formation and Mixing of Two-Dimensional Fluids. *Nano Lett.* **2007**, *7*, 1980–1984.
34. Czolkos, I.; Hakonen, B.; Orwar, O.; Jesorka, A. High-Resolution Micropatterned Teflon AF Substrates for Biocompatible Nanofluidic Devices. *Langmuir* **2012**, *28*, 3200–3205.
35. Elliott, J. T.; Burden, D. L.; Woodward, J. T.; Sehgal, A.; Douglas, J. F. Phospholipid Monolayers Supported on Spun-Cast Polystyrene Films. *Langmuir* **2003**, *19*, 2275–2283.
36. Woodward, J. T.; Meuse, C. W. Mechanism of Formation of Vesicle Fused Phospholipid Monolayers on Alkanethiol Self-Assembled Monolayer Supports. *J. Colloid Interface Sci.* **2009**, *334*, 139–145.
37. Baoukina, S.; Monticelli, L.; Risselada, H. J.; Marrink, S. J.; Tieleman, D. P. The Molecular Mechanism of Lipid Monolayer Collapse. *Proc. Natl. Acad. Sci. U.S.A.* **2008**, *105*, 10803–10808.
38. Czolkos, I.; Guan, J.; Orwar, O.; Jesorka, A. Flow Control of Thermotropic Lipid Monolayers. *Soft Matter* **2011**, *7*, 6926–6933.
39. Erkan, Y.; Halma, K.; Czolkos, I.; Jesorka, A.; Dommersnes, P.; Kumar, R.; Brown, T.; Orwar, O. Controlled Release of Chol-TEG-DNA from Nano- and Micropatterned SU-8 Surfaces by a Spreading Lipid Film. *Nano Lett.* **2008**, *8*, 227–231.
40. Korinek, P. M. Amorphous Fluoropolymers—A New Generation of Products. *Macromol. Symp.* **1994**, *82*, 61–65.
41. Zhang, H.; Weber, S. G. Teflon AF Materials. In *Fluorous Chemistry*; Horvath, I. T., Ed.; Springer-Verlag: Berlin, 2012; Vol. 308, pp 307−337.
42. Resnick, P. R.; Buck, W. H. Teflon® AF: A Family of Amorphous Fluoropolymers with Extraordinary Properties. In *Fluoropolymers 2*; Springer: Berlin, 2002; pp 25−33.
43. Costela, A.; Garciamoreno, I.; Florido, F.; Figuera, J. M.; Sastre, R.; Hooker, S. M.; Cashmore, J. S.; Webb, C. E. Laser-Ablation of Polymeric Materials at 157 nm. *J. Appl. Phys.* **1995**, *77*, 2343–2350.
44. Miyoshi, N.; Oshima, A.; Urakawa, T.; Fukutake, N.; Nagai, H.; Gowa, T.; Takasawa, Y.; Takahashi, T.; Numata, Y.; Katoh, T.; et al. Nano- and Micro-fabrication of Perfluorinated Polymers Using Quantum Beam Technology. *Radiat. Phys. Chem.* **2011**, *80*, 230–235.
45. Fukutake, N.; Miyoshi, N.; Takasawa, Y.; Urakawa, T.; Gowa, T.; Okamoto, K.; Oshima, A.; Tagawa, S.; Washio, M. Micro- and Nano-scale Fabrication of Fluorinated Polymers by Direct Etching Using Focused Ion Beam. *Jpn. J. Appl. Phys.* **2010**, 49.
46. Katoh, T.; Nishi, N.; Fukagawa, M.; Ueno, H.; Sugiyama, S. Direct Writing for Three-Dimensional Microfabrication Using Synchrotron Radiation Etching. *Sens. Actuators, A* **2001**, *89*, 10–15.
47. Kobayashi, A.; Oshima, A.; Okubo, S.; Tsubokura, H.; Takahashi, T.; Oyama, T. G.; Tagawa, S.; Washio, M. Thermal and Radiation Process for Nano-/Micro-fabrication of Crosslinked PTFE. *Nucl. Instrum. Methods Phys. Res., Sect. B* **2013**, *295*, 76–80.
48. Karre, V.; Keathley, P. D.; Guo, J.; Hastings, J. T. Direct Electron-Beam Patterning of Teflon AF. *IEEE Trans. Nanotechnol.* **2009**, *8*, 139–141.
49. Popovici, D.; Sacher, E.; Meunier, M. Photodegradation of Teflon AF1600 during XPS Analysis. *J. Appl. Polym. Sci.* **1998**, *70*, 1201–1207.
50. Hategan, A.; Law, R.; Kahn, S.; Discher, D. E. Adhesively-Tensed Cell Membranes: Lysis Kinetics and Atomic Force Microscopy Probing. *Biophys. J.* **2003**, *85*, 2746–2759.
51. Karlsson, A.; Karlsson, R.; Karlsson, M.; Cans, A. S.; Stromberg, A.; Ryttsen, F.; Orwar, O. Molecular Engineering—Networks of Nanotubes and Containers. *Nature* **2001**, *409*, 150–152.
52. Jesorka, A.; Stepanyants, N.; Zhang, H. J.; Ortmen, B.; Hakonen, B.; Orwar, O. Generation of Phospholipid Vesicle−Nanotube Networks and Transport of Molecules Therein. *Nat. Protoc.* **2011**, *6*, 791–805.
53. Karlsson, M.; Nolkrantz, K.; Davidson, M. J.; Stromberg, A.; Ryttsen, F.; Akerman, B.; Orwar, O. Electroinjection of Colloid Particles and Biopolymers into Single Unilamellar Liposomes and Cells for Bioanalytical Applications. *Anal. Chem.* **2000**, *72*, 5857–5862.